

Increase in observed net carbon dioxide uptake by land and oceans during the past 50 years

A. P. Ballantyne^{1,†}, C. B. Alden², J. B. Miller^{3,4}, P. P. Tans⁴ & J. W. C. White^{1,2}

One of the greatest sources of uncertainty for future climate predictions is the response of the global carbon cycle to climate change¹. Although approximately one-half of total CO₂ emissions is at present taken up by combined land and ocean carbon reservoirs², models predict a decline in future carbon uptake by these reservoirs, resulting in a positive carbon–climate feedback³. Several recent studies suggest that rates of carbon uptake by the land^{4–6} and ocean^{7–10} have remained constant or declined in recent decades. Other work, however, has called into question the reported decline^{11–13}. Here we use global-scale atmospheric CO₂ measurements, CO₂ emission inventories and their full range of uncertainties to calculate changes in global CO₂ sources and sinks during the past 50 years. Our mass balance analysis shows that net global carbon uptake has increased significantly by about 0.05 billion tonnes of carbon per year and that global carbon uptake doubled, from 2.4 ± 0.8 to 5.0 ± 0.9 billion tonnes per year, between 1960 and 2010. Therefore, it is very unlikely that both land and ocean carbon sinks have decreased on a global scale. Since 1959, approximately 350 billion tonnes of carbon have been emitted by humans to the atmosphere, of which about 55 per cent has moved into the land and oceans. Thus, identifying the mechanisms and locations responsible for increasing global carbon uptake remains a critical challenge in constraining the modern global carbon budget and predicting future carbon–climate interactions.

Coupled climate/carbon-cycle models predict decreased carbon (C) uptake by the land, owing to diminishing productivity and increasing respiration, and decreased C uptake by the ocean, associated with acidification, changes in ocean mixing and increasing sea surface temperatures, within this century³. Although detecting changes in regional C sinks is very challenging, several recent studies suggest that C uptake by the land and ocean may already be tapering off or declining. However, diminished C uptake in these studies is often limited to the regional^{5,7–9} or decadal scale^{4,6,10}. In addition, trends in sink intensity in these studies are inferred from satellite measurements⁶, simulated using models^{8,10} or estimated on the basis of inventories of existing C sinks^{4,7,9}. Thus, their implications for long-term variation in the global C budget remain uncertain. Here we focus strictly on global-scale observations provided by atmospheric CO₂ measurements and CO₂ emission estimates, and include the full range of uncertainties in each to estimate changes in global C uptake during the past 50 yr. Although this ‘top-down’ approach does not provide the detailed process-level information of previous studies, it does provide an unbiased assessment of changes in global C uptake.

The growth rate of atmospheric CO₂

$$\frac{dC}{dt} = \sum F + \sum N \quad (1)$$

varies in response to one-way fluxes to the atmosphere (ΣF) and net exchange between the Earth’s surface reservoirs and atmosphere (ΣN). The one-way fluxes include those from fossil fuel emissions, including cement production (F_F), and those from land-use change (F_L).

Negative ΣN values represent net uptake of CO₂ and comprise contributions by the land (N_L) and the oceans (N_O). From the observed atmospheric growth rate and estimated fluxes, we can calculate net global CO₂ uptake ($\Sigma N = dC/dt - \Sigma F$) and the airborne fraction ($AF = (dC/dt)/\Sigma F$). Although both F_F and F_L are often included in calculating AF and ΣN , it can be argued that only F_F should be included in these calculations because it represents the addition of truly extrinsic C to the modern C cycle, which will be redistributed between the atmosphere, oceans and land. We calculate two versions of ΣN and AF, one with F_F and F_L (Figs 1 and 2 and Table 1), and one with only F_F (Table 1).

A major difficulty in characterizing the uncertainty of trends in ΣN and AF is that dC/dt errors are negatively autocorrelated in successive years, whereas ΣF errors are positively autocorrelated. The uncertainty of a trend will be overestimated if the negative autocorrelation is not taken into account in the analysis, and will be underestimated if the positive autocorrelation is not taken into account. Thus, calculations of ΣN and AF contain both positive and negative autocorrelations, the balance of which is time dependent. Before 1980 uncertainties in ΣN and AF are dominated by dC/dt errors, whereas towards the end of the record uncertainties in ΣN and AF become increasingly dominated by ΣF . To take this error structure properly into account, we used a Monte-Carlo-type approach to simulate the errors. To evaluate the

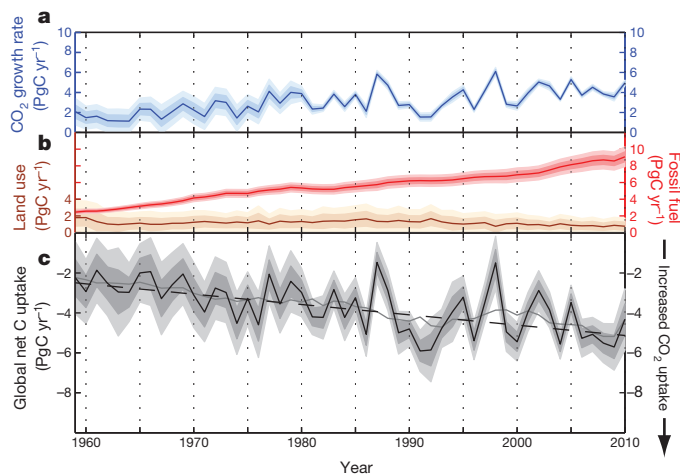


Figure 1 | Trends in the global carbon budget from 1959 to 2010. **a**, The annual atmospheric CO₂ growth rate (dC/dt). **b**, Fluxes of C to the atmosphere from fossil fuel emissions (F_F) are plotted in red and those from land-use changes (F_L) are plotted in brown. **c**, Annual global net C uptake (ΣN) is plotted as a black solid line and is compared with the 10-yr moving average (dark grey line) and the significant linear trend (dashed line) (Table 1). All dark shaded bands represent 1 σ uncertainties and all light shaded bands represent 2 σ uncertainties. Note that the scale of the y axis in **c** has been expanded.

¹Department of Geology, University of Colorado, Boulder, Colorado 80309, USA. ²Institute of Arctic and Alpine Research, University of Colorado, Boulder, Colorado 80309, USA. ³Cooperative Institute for Research in Environmental Sciences, University of Colorado, Boulder, Colorado 80309, USA. ⁴Earth System Research Laboratory, National Oceanographic and Atmospheric Administration, Boulder, Colorado 80305, USA. †Present address: Department of Ecosystem and Conservation Sciences, University of Montana, Missoula, Montana 59812, USA.

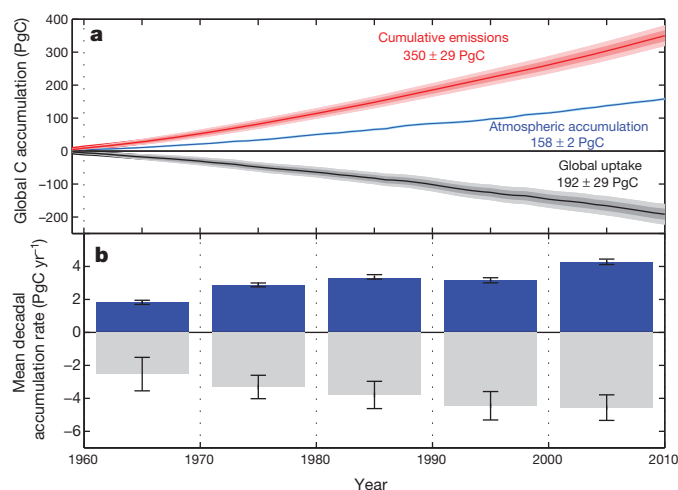


Figure 2 | Accumulation of carbon emissions in the atmosphere, on land and in the oceans. **a**, Sums of emissions from fossil fuels and land-use change integrated from 1959 to 2010 (red) are compared with atmospheric accumulation (blue) and cumulative global uptake (black) by the land and oceans. The dark shaded bands represent 1σ uncertainties and the light shaded bands represent 2σ uncertainties. **b**, Mean decadal C accumulation rates for the atmosphere (blue) and mean global C uptake rates (grey) are calculated as the sum of C accumulation over a given decade divided by 10 yr. Error bars represent the 2σ uncertainties (Methods).

uncertainty in dC/dt since 1980, atmospheric sampling sites were resampled and global mean growth rates were calculated to account for the spatial variability and sparse sampling of atmospheric CO_2 , which contribute much more to uncertainty than do measurement and calibration errors. Before 1980, a negatively autocorrelated error component was added to dC/dt simulations. To assess the uncertainty in ΣF , we combined three independent inventories of F_F emissions^{14–16} with three independent inventories of F_L emissions^{17–19}. To each emission inventory, we added positively autocorrelated random errors to account for temporally persistent accounting errors²⁰. These ΣF emission scenarios were then combined with the simulations of dC/dt to estimate trends in ΣN and AF (Methods).

Significantly increasing linear trends in observed dC/dt (0.054 ± 0.011 billion tonnes of carbon (PgC) per year per year) and estimated F_F (0.115 ± 0.011 PgC yr⁻²) are evident, whereas F_L shows a slight decline between 1959 and 2010 (Fig. 1 and Table 1). Whereas the uncertainty in dC/dt has decreased over time, owing to the addition of network sites monitoring global atmospheric CO_2 , the uncertainty in F_F has increased over time, primarily as a result of growing emissions and a greater contribution from emerging economies. We find a significant negative trend in ΣN of -0.052 ± 0.026 PgC yr⁻² (Fig. 1c and Table 1), indicating a large increase in net global C uptake during the past 50 yr. Net global C uptake has grown on average by 0.5 PgC yr⁻¹ per decade, from 2.4 ± 0.8 PgC yr⁻¹ in 1960 to 5.0 ± 0.9 PgC yr⁻¹ in 2010.

Superimposed on this increasing trend in net global C uptake is considerable variability (Fig. 1c). Although net global C uptake

increased steadily from 1960 to about 1990, substantial oscillations in net global C uptake have occurred over the past 20 yr. In fact, an increasing trend in ΣN of 0.21 ± 0.10 PgC yr⁻² was observed during the 1990s, but this was followed by an equally large decreasing trend in ΣN of -0.19 ± 0.08 PgC yr⁻² since 2000. Thus, it might be inferred that global C sinks diminished during the 1990s; however, this apparent trend is mainly due to the timing of the eruption of Mt Pinatubo in 1991, which enhanced net global C uptake, and the strong El Niño event in 1998, which diminished net global C uptake¹¹.

A commonly used diagnostic for detecting changes in the relative C sink efficiency is the airborne fraction, AF. Our analysis reveals that trends in AF are highly sensitive to whether land-use emissions are included in the global C budget. When only fossil fuel emissions are included, there is a significant decreasing trend in AF, indicating an increase in uptake efficiency. In contrast, when both land-use and fossil fuel emissions are included, the sign of the rate of change of AF switches and the uncertainty range is larger, including both positive and negative trends (Table 1). There has been considerable debate as to whether AF has changed over time and what changes in AF indicate^{12,13,21,22}. Our results show that when land-use emissions are included, there is no detectable change in AF over the last 50 yr. Our findings are corroborated by a recent independent analysis showing no significant change in AF since 1850¹². Moreover, it has been demonstrated that large changes in uptake efficiency are required to alter AF significantly¹³. Thus, changes in AF over time are highly sensitive to land-use emissions and are difficult to interpret, whereas the significant trend in ΣN provides unequivocal evidence that net global CO_2 uptake continues to increase.

Alternatively, we investigate where anthropogenic emissions have accumulated between 1959 and 2010. Approximately 60 PgC from land use and 290 PgC from fossil fuels have been emitted to the atmosphere, making a total of 350 ± 29 PgC of anthropogenic emissions during that time frame (Fig. 2a). Of these, 158 ± 2 PgC remain in the atmosphere and 192 ± 29 PgC have accumulated in combined land and ocean reservoirs. Thus, 55% of anthropogenic CO_2 emissions have been transferred to the land and oceans, and 45% have remained in the atmosphere. The mean decadal C accumulation rate (Fig. 2b) in land and oceans has increased every decade, from 2.5 ± 1.0 PgC yr⁻¹ during the 1960s to 4.6 ± 0.7 PgC yr⁻¹ since 2000. In the atmosphere, the average decadal accumulation has increased from 1.8 ± 0.12 PgC yr⁻¹ during the 1960s to 4.1 ± 0.06 PgC yr⁻¹ between 2000 and 2010. Although the 1990s seem to be anomalous, in that a much greater proportion of C accumulated on land and in the oceans than in the atmosphere, since 2000 the rate of accumulation in the atmosphere has accelerated.

Because the trend in ΣN shows an increase in net global C uptake, N_L and N_O cannot both be decreasing. If regional ocean and land C sinks are indeed diminishing^{5,7–9}, then to satisfy the global C mass balance, these reduced sinks must be more than compensated for by an increase in the rate of uptake by existing C sinks or the formation of new C sinks. A global inventory of C dynamics in established forests has identified strong regional differences in uptake but a fairly constant global average uptake rate of approximately 2.5 PgC yr⁻¹ over the past

Table 1 | Trend analyses of parameters and diagnostics of the global C budget (equation (1)) from 1959 to 2010

Parameters and diagnostics	Slope trend* (PgC yr ⁻²)	95% confidence interval (PgC yr ⁻²)	
		Minimum	Maximum
dC/dt	0.054	0.043	0.065
F_F	0.115	0.103	0.126
F_L	-0.007	-0.041	0.027
AF with F_F only	-0.0016	-0.0029	-0.0002
AF with F_F and F_L	0.0012	-0.0008	0.0032
ΣN with F_F only	-0.063	-0.076	-0.051
ΣN with F_F and F_L	-0.052	-0.077	-0.026

The mean values of slope trend and their 95% confidence interval are calculated from the distribution of simulations (Methods). Significant trends are in bold.

*AF is dimensionless.

20 yr (ref. 4). Similarly, trends in the partial pressure of CO₂ in the ocean indicate a decrease in C uptake in the Atlantic and an increase in C uptake in the Pacific over the past 30 yr (ref. 10). Thus, evidence for a change in the rate of C uptake by existing regional C sinks on land and in the ocean is equivocal. It has been suggested that widespread drought in the Southern Hemisphere has led to a decrease in terrestrial CO₂ uptake⁶ and that increased surface wind velocity has led to decreased CO₂ uptake in the Southern Ocean⁸. Unfortunately, the atmospheric CO₂ observations required to validate these reported declines in Southern Hemisphere CO₂ uptake remain scarce.

From a global mass balance perspective, net uptake of atmospheric CO₂ has continued to increase during the past 50 yr and seems to remain strong. Although present predictions indicate diminished C uptake by the land and oceans in the coming century, with potentially serious consequences for the global climate, as of 2010 there is no empirical evidence that C uptake has started to diminish on the global scale. Therefore, to improve our understanding of carbon–climate interactions, more process studies focusing on mechanisms and regions of increased net CO₂ uptake are required, uncertainty in the global C budget must be reduced by better constraining estimates of fossil fuel emissions, and the global network monitoring atmospheric CO₂ must be expanded to include regions where C uptake is sensitive to climate variability. A fully comprehensive and credible global carbon budget can be achieved only when regional process studies are confirmed by global-scale observations.

METHODS SUMMARY

We use a Monte Carlo approach to assess uncertainty because it permits us to simulate the time-dependent autocorrelation structure of the uncertainty. From 1980 to 2010, the global atmospheric CO₂ growth rate (dC/dt) is calculated from annual differences in mean concentration from an array of selected marine boundary layer sites. To estimate the uncertainty in dC/dt due to site selection, we construct 100 bootstrap simulations of alternative observing networks. The pre-1980 value of dC/dt is calculated as the annual difference in mean concentration at Mauna Loa and the South Pole, with an error structure derived from comparison with the contemporary marine boundary layer network extended back to 1959 (Methods).

For F_F , we use emission estimates from three global inventories—the Carbon Dioxide Information Analysis Center, BP and the Emissions Database for Global Atmospheric Research—to incorporate possible biases that may persist through the entire record, such as energy-to-carbon conversion factors. Each emission inventory is divided into two groups, developed nations (members of the Organization for Economic Co-operation and Development) and developing nations (non-members). The 2σ error for F_F is then estimated as 5% of emissions for all developed nations and 10% of emissions for all developing nations²⁰.

For F_L , we use three independent inventories derived from model simulations of land-use and forest statistics^{17,18,19}, and assign a 2σ error of 50% to each F_L inventory. Because F_F and F_L inventory errors do not vary randomly from year to year, we simulate the uncertainty by generating 500 time series of autocorrelated errors (persistence of ~20 yr) for each inventory. For the case with only F_F we combine the three F_F inventories, and for the case with both F_F and F_L we combine each of our F_F inventories with each of our F_L inventories into a 3×3 matrix of emission scenarios, for a total of 4,500 ΣF emission simulations ($N = 3 \times 3 \times 500 = 4,500$). Values of AF and ΣN were calculated by combining each simulation of ΣF with a randomly chosen simulation of dC/dt. Unless otherwise noted, all uncertainty ranges correspond to 2σ .

Full Methods and any associated references are available in the online version of the paper at www.nature.com/nature.

Received 6 October 2011; accepted 6 June 2012.

1. Meehl, G. A. *et al.* in *Climate Change 2007: The Physical Science Basis* (eds Solomon, S. *et al.*) 792–802 (Cambridge Univ. Press, 2007).
2. Schimel, D. S. *et al.* Recent patterns and mechanisms of carbon exchange by terrestrial ecosystems. *Nature* **414**, 169–172 (2001).
3. Friedlingstein, P. *et al.* Climate-carbon cycle feedback analysis: results from the C4MIP model intercomparison. *J. Clim.* **19**, 3337–3353 (2006).
4. Pan, Y. *et al.* A large and persistent carbon sink in the world's forests. *Science* **333**, 988–993 (2011).
5. Piao, S. *et al.* Net carbon dioxide losses of northern ecosystems in response to autumn warming. *Nature* **451**, 49–52 (2008).
6. Zhao, M. & Running, S. W. Drought-induced reduction in global terrestrial net primary production from 2000 through 2009. *Science* **329**, 940–943 (2010).
7. McKinley, G. A., Fay, A. R., Takahashi, T. & Metzl, N. Convergence of atmospheric and North Atlantic carbon dioxide trends on multidecadal timescales. *Nature Geosci.* **4**, 606–610 (2011).
8. Le Quéré, C. *et al.* Saturation of the Southern Ocean CO₂ sink due to recent climate change. *Science* **316**, 1735–1738 (2007).
9. Schuster, U. & Watson, A. J. A variable and decreasing sink for atmospheric CO₂ in the North Atlantic. *J. Geophys. Res.* **112**, C11006 (2007).
10. Le Quéré, C., Takahashi, T., Buitenhuis, E. T., Rödenbeck, C. & Sutherland, S. C. Impact of climate change and variability on the global oceanic sink of CO₂. *Glob. Biogeochem. Cycles* **24**, GB4007 (2010).
11. Sarmiento, J. L. *et al.* Trends and regional distributions of land and ocean carbon sinks. *Biogeosciences* **7**, 2351–2367 (2010).
12. Knorr, W. Is the airborne fraction of anthropogenic CO₂ emissions increasing? *Geophys. Res. Lett.* **36**, L21710 (2009).
13. Gloor, M., Sarmiento, J. L. & Gruber, N. What can be learned about carbon cycle climate feedbacks from the CO₂ airborne fraction? *Atmos. Chem. Phys.* **10**, 7739–7751 (2010).
14. Boden, T. A., Marland, G. & Andres, R. J. Global, regional, and national fossil-fuel CO₂ emissions. *Carbon Dioxide Information Analysis Center* <http://cdiac.ornl.gov/trends/emis/overview.html> (2010).
15. BP. *Statistical Review of World Energy* <http://www.bp.com/sectionbodycopy.do?categoryId=7500&contentId=7068481> (2011).
16. European Commission. Emissions Database for Global Atmospheric Research (EDGAR). *Europa - EDGAR Overview* <http://edgar.jrc.ec.europa.eu/overview.php?v=40> (2009).
17. Friedlingstein, P. *et al.* Update on CO₂ emissions. *Nature Geosci.* **3**, 811–812 (2010).
18. Stocker, B., Strassmann, K. & Joos, F. Sensitivity of Holocene atmospheric CO₂. *Biogeosciences* **7**, 921–952 (2011).
19. Yang, X., Richardson, T. K. & Jain, A. K. Contributions of secondary forest and nitrogen dynamics to terrestrial carbon uptake. *Biogeosciences* **7**, 3041–3050 (2010).
20. Marland, G., Hamal, K. & Jonas, M. How uncertain are estimates of CO₂ emissions? *J. Ind. Ecol.* **13**, 4–7 (2009).
21. Canadell, J. G. *et al.* Contributions to accelerating atmospheric CO₂ growth from economic activity, carbon intensity, and efficiency of natural sinks. *Proc. Natl Acad. Sci. USA* **104**, 18866–18870 (2007).
22. Le Quéré, C. *et al.* Trends in the sources and sinks of carbon dioxide. *Nature Geosci.* **2**, 831–836 (2009).

Acknowledgements A.P.B. was supported by the US National Research Council and the US National Science Foundation. This manuscript benefitted from comments from J. Neff, N. Lovenduski and G. Marland. We also thank K. Masarie for performing the bootstrap calculations on the atmospheric CO₂ sampling network. This work would not have been possible without the careful measurements made by scientists at NOAA ESRL and volunteer sample collectors throughout the world.

Author Contributions All authors identified the need for this analysis. P.P.T. and J.B.M. contributed to the uncertainty analysis, and P.P.T. and A.P.B. devised the Monte Carlo simulations. A.P.B. and C.B.A. wrote the paper with assistance from all other co-authors.

Author Information Reprints and permissions information is available at www.nature.com/reprints. The authors declare no competing financial interests. Readers are welcome to comment on the online version of this article at www.nature.com/nature. Correspondence and requests for materials should be addressed to A.P.B. (apballantyne@gmail.com).

METHODS

The global annual growth rates (dC/dt) and uncertainties for 1980 to 2010 were calculated for approximately 40 marine boundary layer (MBL) sites from the NOAA/ESRL flask network (<http://www.esrl.noaa.gov/gmd/ccgg/>). These sites are called 'background' sites because they provide access to well-mixed air that is not significantly influenced by nearby sources and sinks of CO_2 . Thus, they have low noise and are representative of large upwind areas. Global averages representative of the MBL were calculated following the method in ref. 23. Annual growth rates were calculated by subtracting mean values of December and January (MDJ) from MDJ values of the following year. The uncertainty in the annual growth rate is dominated by having only 40 sites, each of which may have temporal gaps in its record. We use a bootstrap method to simulate this uncertainty, by repeating the above procedure 100 times. For each realization of a network, 40 sites were randomly selected with replacement from the actual sites, so that some sites are missing whereas others are represented more than once, but always with at least one Arctic, one tropical, one Antarctic, one North Atlantic and one North Pacific site selected. On average, the annual growth rate uncertainty (2σ) is 0.38 PgC yr^{-1} . Analysis of the bootstrap results revealed modest positive autocorrelation coefficients for MDJ errors, of 0.244 and 0.086 for lags of 1 yr and 2 yr, respectively, and strong negative autocorrelation coefficients for dC/dt errors, of -0.413 , -0.166 and -0.085 for lags of 1 yr, 2 yr and 3 yr, respectively. An MDJ value that is too high tends to produce an estimate of dC/dt that is too high for the preceding year and too low for the following year. For the period before 1980, global MDJ values were calculated from the average MDJ of Mauna Loa and South Pole (MLOSP0), with correction for a bias relative to the global MBL mean (see below), and added autocorrelated noise $x_{(t)} = b[0.244x_{(t-1)} + 0.086x_{(t-2)} + \varepsilon_{(t)}]$. Here t denotes the time in years, 0.244 and 0.086 are the 1-yr and 2-yr lag autocorrelation coefficients from above, ε is normally distributed random noise and b is a constant to normalize x so as to have a standard deviation of 0.24 p.p.m. This standard deviation is based on the comparison of MLOSP0 and the global mean MDJ values for the overlapping period, 1980–2010. The monthly mean MLOSP0 data before 1974 are from the Scripps Institution of Oceanography²⁴. The annual growth rates before 1980 are also determined as the differences between successive MDJ values, leading to a 2σ uncertainty of 0.83 PgC yr^{-1} for those years.

The uncertainty in the observed decadal average growth rate is due to the uncertainty in the global MDJ values at the beginning and end of the decade, and also to the uncertainty related to potential drift over the 10-yr period of the reference gas calibration scale (www.esrl.noaa.gov/gmd/ccl/). The latter is negligible compared with the MDJ values. Since 1990 the uncertainty in the decadal average annual growth rate has been 0.07 PgC yr^{-1} , and before 1980 it was 0.12 PgC yr^{-1} . The uncertainty in the observed cumulative CO_2 increase during 1959–2010 is due to the sampling uncertainty of MDJ values in 1959 and MDJ values in 2011, and to potential changes of the measurement calibration. A comparison between MLOSP0 and the MBL average during 1980–2010 shows that MLOSP0 is biased low by an amount that depends on the global rate of fossil fuel emissions (in parts per million, $\text{MLOSP0} - \text{MBL} = -0.035 - 0.072F_F$), with an error of $\sim 0.3 \text{ p.p.m.}$ in 1959. All MLOSP0 values before 1980 were bias-corrected. The Scripps calibration scale, which was used for the period 1958–1995, may have been different from the current World Meteorological Organization scale by as much as 0.3 p.p.m. , and pressure-broadening corrections of instruments²⁵ contributes an additional uncertainty of 0.2 p.p.m. to the calibration. Thus, the uncertainty in the observed cumulative increase during 1959–2010 is probably less than 2 PgC .

Atmospheric CO_2 concentrations are converted from parts per million to petagrams of carbon by using the conversion factor $2.124 \text{ PgC p.p.m.}^{-1}$. This conversion factor implicitly assumes that the annual increases we calculate for the MBL are representative of the entire atmosphere. This assumption may lead to biases in our analysis for two reasons. First, in the continental boundary layer (CBL) CO_2 concentrations tend to be several parts per million higher on average because almost all fossil fuel burning takes place on the continents, despite net uptake by the terrestrial biosphere. Second, mean annual CO_2 concentrations tend to be slightly ($\sim 0.2 \text{ p.p.m.}$) lower in the free troposphere than in the MBL of the Northern Hemisphere and are certainly lower in the stratosphere, where the ongoing CO_2 increase lags the MBL. For a mass-averaged lag of 1.5 yr (ref. 26) of the global stratosphere above 200 mbar ($\sim 20\%$ of the atmosphere) and an

annual growth rate of 2.0 p.p.m. , the stratosphere would be lower than the troposphere by $1.5 \times 2.0 = 3 \text{ p.p.m.}$ Assuming that the MBL can represent the full column produces a high bias of 0.6 p.p.m. ($20\% \times 3 \text{ p.p.m.}$), and one proportionally less when the growth rate was lower. Analysis of the observationally constrained CarbonTracker global mole fraction fields (<http://www.esrl.noaa.gov/gmd/ccgg/carbontracker/>) show CBL zonal mean CO_2 enhancements of 2–4 p.p.m. over the MBL, resulting in global MBL underestimation of surface CO_2 concentrations of 0.6 p.p.m. For 2003, CarbonTracker estimates a global MBL average of 374.92 p.p.m. and a whole-atmosphere average of 374.96 p.p.m. , suggesting that the CBL – MBL and troposphere–stratosphere biases, both of which are produced by fossil fuel CO_2 emissions, approximately cancel one another. Moreover, because we are dealing here with trends, the absolute values of the bias do not matter as much as their trends.

For F_F , we used values calculated from global emission inventories obtained from the Carbon Dioxide Information Analysis Center¹⁴ (CDIAC) for 1959–2010; BP¹⁵ for 1965–2010, augmented by CO_2 from cement production; and EDGAR¹⁶ for 1970–2010. Data before 1965 and 1970, respectively, were back-filled using CDIAC, and EDGAR inventories have been extended from 2007 to 2010 using energy statistics from BP. The 2σ error for F_F was estimated as 5% of emissions for all nations from the Organization for Economic Cooperation and Development (OECD) and 10% of emissions for all non-OECD nations²⁰. These errors do not vary randomly from year to year. These errors persist for successive years as inventory accounting procedures remain the same, but whenever procedures change retroactive step revisions are introduced over many years. To address this uncertainty, 500 realizations of F_F were created from each of the three inventories, multiplying the original emissions estimates by a time-dependent autoregressive error factor of $1 + cy_{(t)}$, where $y_{(t)} = \text{lag } 1 \times y_{(t-1)} + \varepsilon_{(t)}$, t denotes time in years, lag 1 is the autoregressive coefficient for the previous year's value, ε is normally distributed random noise and c is a constant factor to normalize the resulting 2σ errors to 5 or 10%. We chose lag 1 = 0.95, so that the 'memory' of errors is $\sim 20 \text{ yr}$. As a sensitivity experiment, we increased the uncertainty in F_F emissions to 10% for OECD nations and 20% for non-OECD nations. Although this increase in uncertainty yielded a wider distribution of trends in ΣN , more than 95% of all trends in ΣN were still negative, indicating that the significant trends in ΣN are robust. We note that if we had assumed that errors for individual countries are independent (instead of grouping them into OECD and non-OECD), the uncertainty estimate of the global emissions would be smaller. In reality, there is a lot of communication between countries about their emission accounting procedures. By including autocorrelation in our Monte Carlo simulations, errors are allowed to change slowly over time, so that the relative errors in cumulative emissions are smaller than the stated 5 or 10% annual uncertainties. Errors 20 yr apart can be of opposite sign and may thus partly cancel each other. Errors that persist over the entire record are considered by using three different fossil fuel emission inventories.

For F_L estimates, we used three different inventories of fossil fuel emissions from land-use change. We used the well-established and updated accounting methods in ref. 27, but note that in a recent reanalysis of tropical deforestation rates, emission estimates since 2000 have been revised downward¹⁷. We also used two independent inventories of F_L emissions derived from temporal maps of land-use change combined with climate model simulations^{18,19}. To account for the serial correlation of errors in F_L , we used the same autoregressive error structure as described previously for F_F , except they were normalized to 2σ errors of 50%.

23. Masarie, K. A. & Tans, P. P. Extension and integration of atmospheric carbon dioxide data into a globally consistent measurement record. *J. Geophys. Res.* **100**, 11593–11610 (1995).
24. Keeling, C. D. *et al.* A three dimensional model of atmospheric CO_2 transport based on observed winds: 1. Analysis of observational data. *Geophys. Monogr.* **55**, 165–236 (1989).
25. Griffith, D. W. T., Keeling, C. D., Adams, J. A., Guenther, P. R. & Bacastow, R. B. Calculations of carrier gas effects in non-dispersive infrared analyzers. II. Comparisons with experiment. *Tellus* **34**, 385–397 (1982).
26. Andrews, A. E. *et al.* Empirical age spectra for the midlatitude lower stratosphere from in situ observations of CO_2 : quantitative evidence for a subtropical barrier to horizontal transport. *J. Geophys. Res.* **106**, 10257–10274 (2001).
27. Houghton, R. A. Revised estimates of the annual net flux of carbon to the atmosphere from changes in land use and land management 1850–2000. *Tellus B* **55**, 378–390 (2003).